

Experimental Evidence for Proton Motive Force-Dependent Catalysis by the Diheme-Containing Succinate:Menaquinone Oxidoreductase from the Gram-Positive Bacterium *Bacillus licheniformis*[†]

M. Gregor Madej,[‡] Hamid R. Nasiri,[§] Nicole S. Hilgendorff,[‡] Harald Schwalbe,[§] Gottfried Uden,^{||} and C. Roy D. Lancaster^{*,‡}

Department of Molecular Membrane Biology, Max Planck Institute of Biophysics, Max-von-Laue-Strasse 3, D-60438 Frankfurt am Main, Germany, Institut für Organische Chemie und Chemische Biologie, Center for Biomolecular Magnetic Resonance, Johann Wolfgang Goethe-Universität, Max-von-Laue-Strasse 7, D-60438 Frankfurt am Main, Germany, and Institut für Mikrobiologie und Weinforschung, Johannes Gutenberg-Universität Mainz, Becherweg 15, 55099 Mainz, Germany

Received August 31, 2006; Revised Manuscript Received October 5, 2006

ABSTRACT: In Gram-positive bacteria and other prokaryotes containing succinate:menaquinone reductases, it has previously been shown that the succinate oxidase and succinate:menaquinone reductase activities are lost when the transmembrane electrochemical proton potential, Δp , is abolished by the rupture of the bacteria or by the addition of a protonophore. It has been proposed that the endergonic reduction of menaquinone by succinate is driven by the electrochemical proton potential. Opposite sides of the cytoplasmic membrane were envisaged to be separately involved in the binding of protons upon the reduction of menaquinone and their release upon succinate oxidation, with the two reactions linked by the transfer of two electrons through the enzyme. However, it has previously been argued that the observed Δp dependence is not associated specifically with the succinate:menaquinone reductase. Definitive insight into the mechanism of catalysis of this reaction requires a corresponding functional characterization of an isolated, membrane-bound succinate:menaquinone reductase from a Gram-positive bacterium. Here, we describe the purification, reconstitution into proteoliposomes, and functional characterization of the diheme-containing succinate:menaquinone reductase from the Gram-positive bacterium *Bacillus licheniformis* and, with the help of the design, synthesis, and characterization of quinones with finely tuned oxidation/reduction potentials, provide unequivocal evidence for Δp -dependent catalysis of succinate oxidation by quinone as well as for Δp generation upon catalysis of fumarate reduction by quinol.

Succinate:quinone oxidoreductases (SQORs¹) (1, 2) are integral membrane protein complexes, which couple the two-electron oxidation of succinate to fumarate (succinate \rightarrow fumarate + 2H⁺ + 2e⁻; $E_{M7} = +25$ mV (3)) to the two-electron reduction of quinone to quinol (quinone + 2H⁺ + 2e⁻ \rightarrow quinol) as well as catalyzing the opposite reaction,

the reduction of fumarate by quinol (4). In mitochondria and some aerobic bacteria, succinate:ubiquinone reductase, also known as succinate dehydrogenase from the tricarboxylic acid (TCA or Krebs) cycle and as complex II of the aerobic respiratory chain, catalyzes the mildly exergonic reduction of succinate by ubiquinone (Q, E_{M7} (Q/QH₂) = +90 mV (3)), which is not directly associated with energy storage in the form of a transmembrane electrochemical proton potential (Δp). Gram-positive bacteria do not contain ubiquinone but rather the lower-potential menaquinone (MK (5), E_{M7} (MK/MKH₂) = -74 mV (6)). In these cases, the catalyzed oxidation of succinate by quinone is endergonic under standard conditions (1, 7, 8). Consequently, these bacteria face a thermodynamic problem in supporting the catalysis of this reaction *in vivo*.

In Gram-positive bacteria, such as *Bacillus subtilis* and *Bacillus licheniformis* and other prokaryotes containing succinate:menaquinone reductases, the succinate oxidase and succinate:menaquinone reductase activities are lost when the transmembrane electrochemical proton potential, Δp , is abolished by the rupture of the bacteria or by the addition of a protonophore (7, 8, 9). It has been proposed that the endergonic reduction of menaquinone by succinate is driven by the electrochemical proton potential (8). The protons

[†] This work was supported by the Deutsche Forschungsgemeinschaft (SFB 472 "Molecular Bioenergetics") and the Max Planck Society.

* To whom correspondence should be addressed. Tel: +49-69-6303-1013. Fax: +49-69-6303-1002. E-mail: Roy.Lancaster@mpibp-frankfurt.mpg.de.

[‡] Max Planck Institute of Biophysics.

[§] Johann Wolfgang Goethe-Universität.

^{||} Johannes Gutenberg-Universität Mainz.

¹ Abbreviations: C₁₂E₉, polyoxyethylene 9-dodecyl ether; CCCP, carbonyl cyanide *m*-chloro-phenylhydrazone; DDM: *n*-dodecyl- β -D-maltoside; DMN, 2,3-dimethyl-1,4-naphthoquinone; DMNH₂, 2,3-dimethyl-1,4-naphthoquinol; DTE, dithioerythritol; DTT, dithiothreitol; EMN, 2-ethyl-3-methyl-1,4-naphthoquinone; EMNH₂, 2-ethyl-3-methyl-1,4-naphthoquinol; EQ-0, 2,3-dimethoxy-5-ethyl-6-methyl-1,4-benzoquinone; EQH₂-0, 2,3-dimethoxy-5-ethyl-6-methyl-1,4-benzoquinol; FAD, flavin adenine dinucleotide; Fum, fumarate; HNN, 2-hydroxy-3-neopentyl-1,4-naphthoquinone; MMAN, 2-methyl-3-methylamino-1,4-naphthoquinone; MMANH₂, 2-methyl-3-methylamino-1,4-naphthoquinol; MOPS, 3-[*N*-morpholino] propanesulfonic acid; PL, phospholipid; QFR, quinol:fumarate reductase; SQR, succinate:quinone reductase; SQOR, succinate:quinone oxidoreductase.

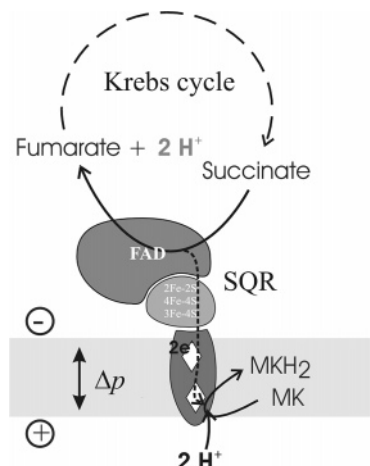


FIGURE 1: Overview of the composition and orientation of the SQR from Gram-positive bacteria and the reaction catalyzed. The SQR subunits are (from top to bottom) A, B, and C. The *b*-type heme groups are indicated by white diamonds. The positive (outside) and negative (inside) sides of the cytoplasmic membrane are indicated.

consumed in the reduction of menaquinone were envisaged to be taken up from outside of the bacteria (8, 10), whereas the protons liberated upon succinate oxidation were released to the cytoplasm (Figure 1). The two reactions are linked by the transfer of two electrons through the enzyme (11, 12). If succinate oxidation by menaquinone were driven at the expense of Δp , the reverse reaction, fumarate reduction by menaquinol, catalyzed by the same enzyme, should generate a Δp across the membrane. The latter has indeed been shown in the case of *B. subtilis* cells and isolated membranes containing succinate:menaquinone reductase (13). However, it has been argued that the observed effect is not associated specifically with the succinate:menaquinone reductase (14). Clearly, definitive insight into the mechanism of catalysis of this intriguing reaction requires a corresponding functional characterization of an isolated, membrane-bound succinate:menaquinone reductase from a Gram-positive bacterium. Here, we describe the purification, reconstitution into proteoliposomes, and functional characterization of the succinate:quinone reductase from the Gram-positive bacterium *Bacillus licheniformis* and provide unequivocal evidence for Δp -dependent catalysis of succinate oxidation by quinone as well as Δp generation upon fumarate reduction by quinol.

EXPERIMENTAL PROCEDURES

Cell Growth, Harvest, Enzyme Preparation, and the Preparation of Proteoliposomes. Cells of *Bacillus licheniformis* (DSM 13) were grown in White medium (15), with 40 mM succinate as the C-source under aerobic conditions to $OD_{578\text{nm}} = 2.1$ as described in ref 8 (8), harvested, and suspended in 30 mM K-phosphate buffer (pH 7.0) containing 20 mM MgSO_4 , 2 mM malonate, 2 mM DTT, and 0.1 mM PMSF. The solution was homogenized in the presence of $0.05 \text{ g} \cdot \text{L}^{-1}$ DNase and $1 \text{ mg} \cdot \text{mL}^{-1}$ lysozyme. The cells were disrupted by sonication (Branson Sonifier 250) output 50%, ($\sim 100 \text{ W}$) $4 \times 5 \text{ min}$ at 0°C in presence of 1 mM EDTA and 1 tablet $\cdot 100 \text{ mL}^{-1}$ Protease inhibitor-cocktail (Roche Diagnostics GmbH). The unbroken cells were removed by centrifugation at $5000g$ for 20 min, yielding a supernatant that was centrifuged at $100\,000g$ for 60 min. The pellet of this centrifugation step was designated as membrane fraction,

resuspended in 25 mM MOPS buffer (pH 7.0), 20 mM MgSO_4 , 5 mM malonate, 2 mM DTT, 2 mM arginine, 1 mM EDTA, 0.1 mM PMSF, and 3% (w/v) C_{12}E_9 (polyoxyethylene 9-dodecyl ether) to a protein concentration of 6.5 mg/mL and left for solubilization under continuous stirring at 6°C for 1 h. Centrifugation at $100\,000g$ for 45 min was performed to remove the unsolubilized material. The supernatant was transferred into 30 mM MOPS (pH 7.0) buffer containing 2 mM malonate, 2 mM DTT, and 0.05% (w/v) C_{12}E_9 (buffer A) by subsequent pressure dialysis (cutoff 100–300 kDa). The material was applied then to a HiLoad Q-Sepharose (Amersham) ion exchange column. The adsorbed protein was eluted by increasing the KCl concentration gradually from 50 to 500 mM. Fractions absorbing at 415 nm were pooled and transferred into 25 mM MOPS (pH 7.0) buffer containing 2 mM malonate, 2 mM DTE, and 0.02% (w/v) DDM (*n*-dodecyl- β -D-maltoside) (buffer B) by pressure dialysis (cutoff 100–300 kDa). This material was applied to a RESOURCE-Q (Amersham) anion exchange column and washed with buffer B over 15 column volumes and eluted with 350 mM KCl. As the last isolation step, a TSK 4000 size exclusion chromatography was performed in buffer B. The eluting fractions that absorbed at 415 nm were pooled and designated as the SQR sample. The proteoliposomes were prepared as described (16, 17) with the exception that SQR from *B. licheniformis* was used. For proteoliposomes prepared under these conditions, it was found that for a membrane protein complex of very similar composition and topology, the proteoliposomes contained the enzyme in a uniform orientation with its hydrophilic subunits oriented solely toward the liposomal exterior (17).

Enzymatic Assays. Quinol oxidation by fumarate was monitored by measuring quinol-specific absorbance differences. For DMNH_2 , the difference at 270 nm minus 290 nm ($\Delta\epsilon_{270-290} = 15.2 \text{ mM}^{-1} \cdot \text{cm}^{-1}$) was used, and for MMANH_2 , the difference at 280 nm minus 320 nm ($A_{280} - A_{320} = 27.6 \text{ mM}^{-1} \cdot \text{cm}^{-1}$) (16) was used. The reduction of EMN was monitored by recording the difference at 270 nm minus 290 nm ($\Delta\epsilon_{270-290} = 15.7 \text{ mM}^{-1} \cdot \text{cm}^{-1}$) and that of EQ-0 by the absorption change at 278 nm ($\epsilon = 14.7 \text{ mM}^{-1} \cdot \text{cm}^{-1}$) (18).

Quinone Synthesis. The syntheses of DMN (19) and MMAN (16) have been described previously. The syntheses of 2,3-dimethoxy-5-ethyl-6-methyl-1,4-benzoquinone (EQ-0), 2-ethyl-3-methyl-1,4-naphthoquinone (EMN), and 2-hydroxy-3-neopentyl-1,4-naphthoquinone (HNN) are described below (see Figure 2 for the respective chemical structures). NMR spectra were recorded on a Bruker spectrometer AM250 operating at a ^1H frequency of 250 MHz. The NMR resonance assignment of carbon atoms were obtained from DEPT135 experiments (20). Elementary analyses were measured on a Foss Heraeus CHN-O-RAPID instrument. IR spectra were recorded on a Perkin-Elmer spectrometer. All reactions were monitored by thin-layer chromatography (TLC), performed on silica gel POLYgram (Macherey-Nagel). Chromatographic purifications were done with Merck silica gel 60. Cyclovoltammetry was measured in dimethoxyethane with tetrabutylammoniumperchlorate as the supporting electrolyte on platinum working and counter electrodes. The oxidation–reduction potentials E_0 are given relative to a Ag/AgCl reference electrode, with a sweep rate of 50 mV/s. We have previously shown that the relative results obtained for different quinones by this procedure (i.e., the differences

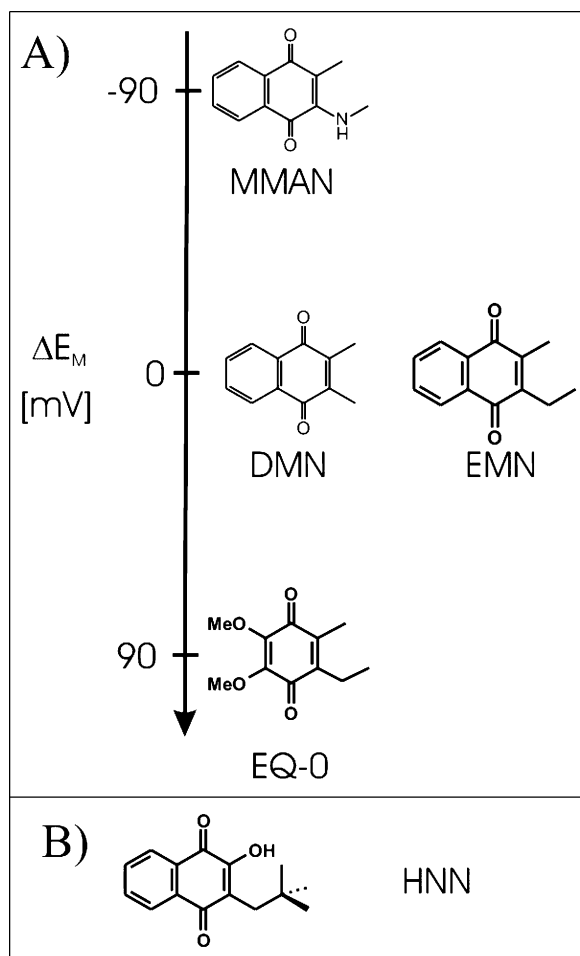


FIGURE 2: Chemical structures of quinones used in this work. (A) 2-Methyl-3-methylamino-1,4-naphthoquinone (MMAN), 2,3-dimethyl-1,4-naphthoquinone (DMN), 2-ethyl-3-methyl-1,4-naphthoquinone (EMN), 2,3-dimethoxy-5-ethyl-6-methyl-1,4-benzoquinone (EQ-0), and the oxidation–reduction midpoint potentials of the associated quinone/quinol pairs relative to that of the DMN/DMNH₂ couple. (B) Inhibitor: 2-hydroxy-3-neopentyl-1,4-naphthoquinone (HNN).

in redox potential between different quinones) are comparable to those obtained by measuring the respective *in situ* redox potentials in the protein (16), provided that the quinones possess similar affinities for the protein. The latter can be concluded to be the case in the present study on the basis of the requirement of similar substrate concentrations for half-maximal catalytic rates (Table 3, below).

2,3-Dimethoxy-5-ethyl-6-methyl-1,4-benzoquinone (EQ-0). The title compound was synthesized starting from commercially available 2,3-dimethoxy-5-methyl-1,4-benzoquinone. The ethyl residue was introduced by a radical Hunsdiecker decarboxylation (21) of propanoic acid using silver nitrate and peroxydisulfate in an acetonitrile/water mixture. A mixture of 1 g (5.43 mmol) of 2,3-dimethoxy-5-methyl-1,4-benzoquinone, 0.48 g (6.51 mmol) of propanoic acid, and 0.25 g (1.45 mmol) of silver nitrate in 30 mL of an acetonitrile/water mixture (5:1) was heated at 80 °C. At this temperature, a solution of 2.8 g (12.5 mmol) of ammonium persulfate in 10 mL of water was slowly added. After 2 h, the mixture was diluted with water and extracted twice with dichloromethane, dried, and concentrated under reduced pressure. The crude product was purified by silica chromatography (hexane/ethylacetate 4:1) to give 0.23 g (20%) of

EQ-0. ¹H NMR (250.13 MHz, CDCl₃): δ (ppm) = 4.00 (s, 6H, 2×OMe₃), 2.49 (dd, J = 6.9 Hz, 2H, CH₂CH₃), 2.03 (s, 3H, CH₃), 1.05 (t, J = 6.9 Hz, 3H, CH₂CH₃). ¹³C NMR (62.9 MHz, CDCl₃): δ (ppm) = 184.7; 183.9 (C=O), 144.4; 144.2; 144.0; 138.4 (C), 19.6 (CH₂), 61.1; 12.9; 11.5 (CH₃). Anal. Calcd for C₁₁H₁₄O₄: C 62.85, H 6.71. Found: C 62.67, H 6.86. IR (KBr pellet) 3286.11; 2974.66; 2946.70; 2252.45; 1648.84; 1611.23; 1457.92; 1272.79; 1071.26; 865.88 cm⁻¹. E_0 = -780 mV, 90 mV higher than that for DMN/DMNH₂ (16).

Synthesis of 2-Ethyl-3-methyl-1,4-naphthoquinone (EMN). The synthesis of the title compound was identical to that of EQ-0. Instead of 2,3-dimethoxy-5-methyl-1,4-benzoquinone, 2-methyl-1,4-naphthoquinone was used. ¹H NMR (250.13 MHz, CDCl₃): δ (ppm) = 8.0 – 7.9 (m, 2H, aromatic protons), 7.6 – 7.5 (m, 2H, aromatic protons), 2.56 (q, J = 7.5 Hz, 2H, CH₂CH₃), 2.10 (s, 3H, CH₃), 1.04 (t, J = 7.5 Hz, 3H, CH₂CH₃). ¹³C NMR (62.9 MHz, CDCl₃): δ (ppm) = 185.3; 184.4 (C=O), 148.5; 142.8; 132.2; 132.1 (C), 133.3, 133.2, 126.2, 126.1 (CH), 20.3 (CH₂), 12.9; 12.3 (CH₃). Anal. Calcd for C₁₃H₁₂O₂: C 77.98, H 6.04. Found: C 77.78, H 6.07. IR (KBr pellet) 3291.89; 2967.91; 2873.42; 1661.37; 1594.84; 1459.85; 1378.85; 1298.82; 791.64; 715.46 cm⁻¹. E_0 = -870 mV, equivalent to that for DMN/DMNH₂ (16).

2-Hydroxy-3-neopentyl-1,4-naphthoquinone (HNN; NSC 102531). The title compound was synthesized by an alkylation/epoxidation and acid-catalyzed epoxide cleavage of 1,4-naphthoquinone. This method was recently successfully applied by us for the synthesis of 2-decyl-3-hydroxy-1,4-naphthoquinone (16). The aliphatic side chain was introduced by radical Hunsdiecker decarboxylation (21) of 3,3-dimethylbutanoic acid using silver nitrate and peroxydisulfate. A mixture of 4 g (25 mmol) of 1,4-naphthoquinone, 3.5 g (30 mmol) of 3,3-dimethylbutanoic acid, and 1 g (6 mmol) of silver nitrate in 60 mL of an acetonitrile/CH₂Cl₂/water mixture (5:5:2) was heated at 80 °C. At this temperature, a solution of 11.4 g (50 mmol) of ammonium persulfate in 20 mL water was slowly added. After 2 h, the mixture was diluted with water and extracted twice with dichloromethane, dried, and concentrated under reduced pressure. The crude product was purified by passing through a pad of silica with hexane/ethylacetate 6:1 as the eluent. Recrystallisation from methanol gave 3.9 g (68.3%) of 2-neopentyl-1,4-naphthoquinone. ¹H NMR (250.13 MHz, CDCl₃): δ (ppm) = 8.1 – 8.0 (m, 2H, aromatic protons), 7.7 – 7.5 (m, 2H, aromatic protons), 6.8 (s, 1H, CH), 2.6 (s, 2H, CH₂), 0.9 (s, 9H, 3×CH₃). ¹³C NMR (62.9 MHz, CDCl₃): δ (ppm) = 185.2; 184.8 (C=O), 149.5; 132.2; 132.1; 32.4 (C), 137.2; 133.6; 133.5; 126.7; 125.8 (CH), 41.6 (CH₂), 29.6 (CH₃). Anal. Calcd. for C₁₅H₁₆O₂: C 78.92, H 7.06. Found: C 78.96, H 7.18.

In the second step, 2-neopentyl-1,4-naphthoquinone was converted to 1a-neopentyl-1a,7a dihydro-naphth[2,3b]oxirene-2,7-dione via Δ^2 -epoxidation. 1 g (4.4 mmol) of 2-neopentyl-1,4-naphthoquinone was dissolved in ethanol (3 mL), and a solution of alkaline hydrogen peroxide (1.5 mL of 30% H₂O₂, 60 mg sodium carbonate in 0.6 mL water) was added. After 1 h of stirring at room temperature, a solution of alkaline hydrogen peroxide was again added, and the reaction was stirred for an additional hour, during which the yellow solution became colorless. The solution was diluted with water and extracted twice with dichloromethane, dried, and

Table 1: Purification Table for the Isolation of *B. licheniformis* SQR^a

	yield protein (mg)	fumarate reduction by DMNH ₂			purification factor
		spec. activity (U·mg ⁻¹)	total activity (U)	total activity (%)	
crude membranes	320	0.8	256	100	1
HiLoad Q anion exchange	54	2.4	129	50.4	3.0
RESOURCE-Q anion exchange	39	2.7	107	41.8	3.4
TSK 4000 gel filtration	11	6.1	67	26.2	7.6

^a One unit (U) corresponds to 1 μ mol of the substrate turned over per minute.

concentrated under reduced pressure to give 0.94 g (88%) of the epoxide. ¹H NMR (250.13 MHz, CDCl₃): δ (ppm) = 8.1 – 7.9 (m, 2H, aromatic protons), 7.8 – 7.7 (m, 2H, aromatic protons), 3.9 (s, 1H, CH), 2.7 (d, J = 14.2 Hz, 1H, CH₂), 1.5 (d, J = 14.2 Hz, 1H, CH₂), 1.0 (s, 9H, 3 \times CH₃). ¹³C NMR (62.9 MHz, CDCl₃) δ (ppm) = 191.7; 190.1 (C=O), 132.0; 131.5; 127.6; 62.8 (C), 134.4; 134.2; 126.9; 126.5; 60.8 (CH), 40.3 (CH₂), 30.9 (CH₃).

In the last step, the epoxide was cleaved under acetic conditions to give the inhibitor 2-hydroxy-3-neopentyl-1,4-naphthoquinone. Then, 0.250 g (1 mmol) of the crude epoxide was dissolved in 1 mL of concentrated sulfuric acid and stirred at room temperature for 10 min. The reaction was diluted with aqueous NaHCO₃ solution and extracted twice with dichloromethane, dried, and concentrated under reduced pressure. The crude product was purified by silica chromatography (hexane/ethylacetate 6:1) to give 0.160 g (64%) of 2-hydroxy-3-neopentyl-1,4-naphthoquinone. ¹H NMR (250.13 MHz, CDCl₃): δ (ppm) = 8.1 – 8.0 (m, 2H, aromatic protons), 7.7 – 7.5 (m, 2H, aromatic protons), 7.3 (s br, 1H, OH), 2.5 (s, 2H, CH₂), 0.9 (s, 9H, 3 \times CH₃). ¹³C NMR (62.9 MHz, CDCl₃) δ (ppm) = 185.0; 181.4 (C=O), 154.0; 133.0; 129.4; 122.9; 33.9 (C), 134.8; 132.8; 126.9; 126.0; (CH), 36.0 (CH₂), 30.2 (CH₃). IR (KBr pellet): 3359.39; 2360.44; 1664.27; 1644.02; 1593.88; 1369.21; 1272.79; 1215.9 cm⁻¹. Anal. Calcd for C₁₅H₁₆O₃: C 73.75, H 6.6. Found: C 74.02, H 6.87.

Acidification Measurements, H⁺/e⁻ Ratio. The acidification measurements in the direction of fumarate reduction were performed as described (16). In experiments monitoring the opposite reaction, in the direction of succinate oxidation, EQ-0 was used instead of MMAN, and the reduction of the quinone prior to the reaction was omitted. The enzymatic reaction was started by the addition of 80 μ M succinate.

Determination of $\Delta\Psi$. The generation of $\Delta\Psi$ during the oxidation of MMANH₂ by fumarate as catalyzed by the SQR was measured as described for measurements on *W. succinogenes* QFR (16). The opposite reaction, the reduction of EQ-0 by succinate, was monitored using a TPP⁺-selective electrode, purchased from Microelectrodes, Inc. (Bedford, USA). Proteoliposomes were suspended in 15 mM HEPES buffer (adjusted to pH 7.5 with NaOH) containing 100 mM KCl. The reaction was started by the addition of succinate. TPP⁺ uptake was calculated from the amplitudes between the succinate addition and the level where the TPP⁺ concentration reached a minimum. $\Delta\Psi$ was calculated as described (17).

RESULTS AND DISCUSSION

In order to establish unambiguously whether the diheme-containing succinate:menaquinone reductases from Gram-

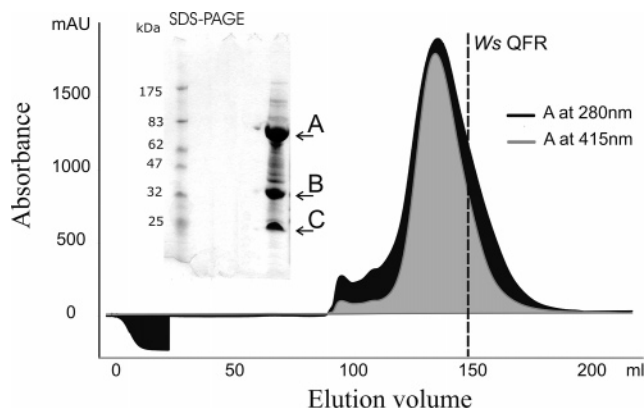


FIGURE 3: TSK 4000 gel filtration elution profile of the SQR from *B. licheniformis*. The black area indicates the absorbance at 280 nm, the superimposed gray area indicates the absorbance of the heme Soret band at 415 nm. For comparison, the elution maximum of the QFR from *W. succinogenes* is indicated by the dashed line. The inset shows the SDS-PAGE of the pooled SQR fractions.

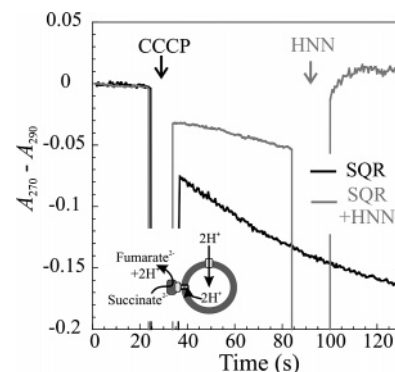


FIGURE 4: Addition of the uncoupler CCCP stimulates the reduction of EMN by succinate as catalyzed by the proteoliposomal SQR. Proteoliposomal SQR was unable to significantly support the reduction of EMN by succinate without the presence of the uncoupler (black trace). This activity could be inhibited by the addition of 60 μ M inhibitor HNN (gray trace with 30 μ M HNN; the addition of further HNN to 60 μ M is indicated by the gray arrow).

positive bacteria operate by specific exploitation of a Δp , the enzyme from *B. licheniformis* was selected after preliminary screening of the respective enzymes from a number of Gram-positive bacteria (Supporting Information, Table S1), purified (Table 1 and Figure 3), reconstituted into proteoliposomes, and characterized (Figures 4–6 and Tables 2 and 3). For this purpose, in addition to the two quinones synthesized previously (DMN (19) and MMAN (16)), two modified quinones (EQ-0 and EMN) and a naphthoquinone inhibitor (HNN) were synthesized and characterized.

Purification and Oligomerization State. The genome sequence of *B. licheniformis* has been determined (22), and

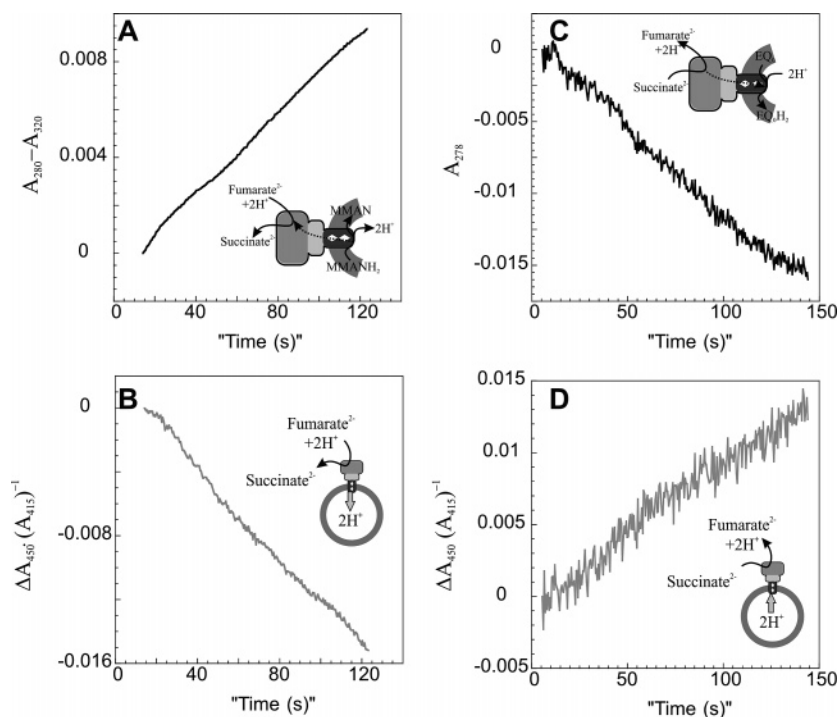


FIGURE 5: Catalytic activity of proteoliposomal SQR from *B. licheniformis*, EQ-0-reduction (A) and MMANH₂ oxidation (C) and the monitoring of the respective generation of Δp H (B and D). Proteoliposomes (200 μ g of phospholipid) containing the SQR and the respective quinone substrate (10 mM/mg phospholipid) were suspended in a N₂-flushed buffer. In the case of MMAN, NaBH₄ was added to reduce the quinone, and the reaction was started by the addition of fumarate (20 μ M). In the case of EQ-0, the reaction was started with succinate (20 μ M), without the previous reduction of the quinone.

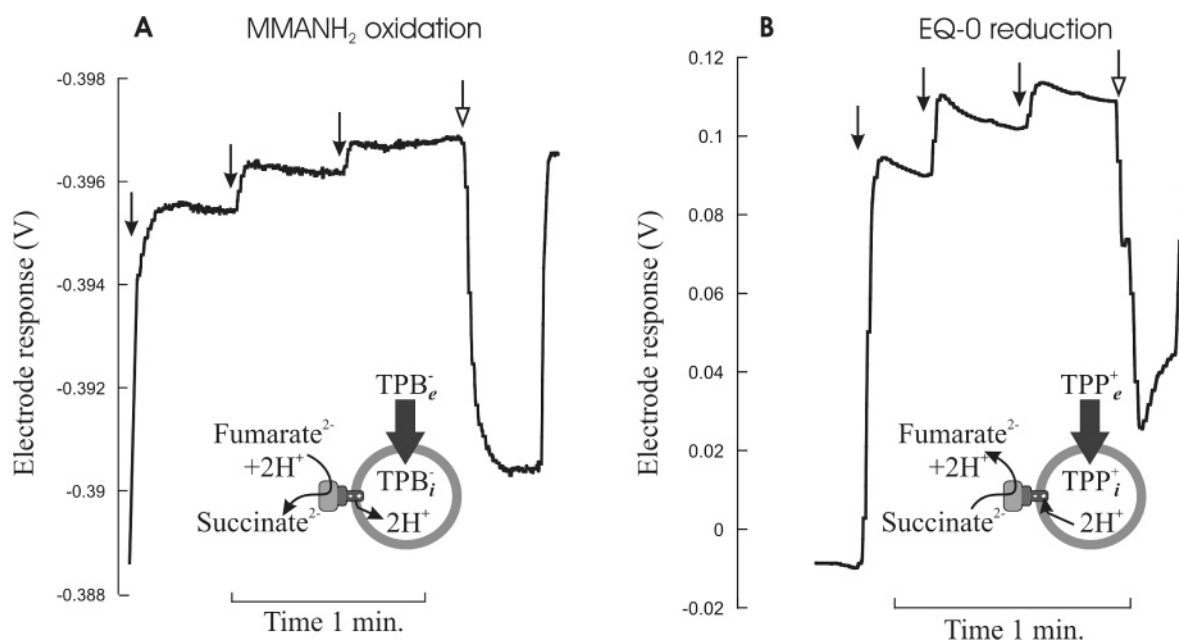


FIGURE 6: TPP⁺ and TPB⁻ accumulation upon (A) EQ-0-reduction and (B) MMANH₂ oxidation. The $\Delta\Psi$ was monitored as the uptake of TPP⁺ (A) or the uptake of TPB⁻ (B) with an electrode sensitive to TPP⁺ or TPB⁻, respectively. Proteoliposomes (400 μ g of phospholipid) containing the SQR and the respective quinone substrate (10 mM/mg phospholipid) were suspended in a N₂-flushed buffer. Prior to the reaction, the electrode was calibrated by the addition of TPP⁺ or TPB⁻ (solid arrows) as annotated in the plot. In the case of MMAN, NaBH₄ was added to reduce the quinone, and the reaction was started by the addition of fumarate (20 μ M; open arrow in panel A). In the case of EQ-0, the reaction was started with succinate (20 μ M; open arrow in panel B), without the previous reduction of the quinone.

the proteins encoded by the *sdhC*, *sdhA*, and *sdhB* genes have the molecular masses of 23, 65, and 28 kDa, respectively, giving the molecular mass of 113 kDa for the heterotrimeric protomer. The enzyme was enriched approximately 8-fold (Table 1). We obtained a homogeneous SQR sample with a specific activity of 6.1 U·mg⁻¹. The retention volume from the gel-filtration column TSK 4000

was 13 mL lower than that of the QFR from *W. succinogenes*, which exists as a homodimer of heterotrimers (23, 24). In our case, the results indicate that SQR from *B. licheniformis* exists as a homotrimeric complex of the heterotrimeric protomer, which is in line with the homotrimers found for the SQR enzymes from *E. coli* (25) and *Corynebacterium glutamicum* (26).

Table 2: Specific Activities (in U/mg) of Succinate Oxidation by EMN as Catalyzed by *B. licheniformis* SQR in the Absence (a) and Presence (b) of 30 μ M HNN

EMN	detergent-solubilized state (in 0.02% DDM)	sealed proteoliposomes	uncoupled proteoliposomes (+25 μ M CCCP)
(a) SQR	6.7	n.d. ^a	8.2
(b) SQR + 30 μ M HNN	3.4	1.4	3.1

^an.d. = not detectable.Table 3: H^+/e^- Ratio Measurements with Proteoliposomes and Associated Specific Activities of *B. licheniformis* SQR Reconstituted into Proteoliposomes

quinol substrate	redox midpoint potential difference (mV) relative to that of DMN/DMNH ₂	direction of e^- transfer	H^+/e^- ratio	specific activity (U·mg ⁻¹ protein)	$S_{0.5}$ ^a (μ M)
MMANH ₂	−90	Q → fumarate	0.8	5.1	73
DMNH ₂	0	Q → fumarate	0	4.8	51
EQ-0	+90	succinate → Q	0.9	7.4	83

^a $S_{0.5}$ is the substrate concentration at which the half-maximal rate is observed.

Inhibitor Synthesis and Characterization. We found a new synthetic route for 2-hydroxy-3-neopentyl-1,4-naphthoquinone (HNN) by an alkylation/epoxidation and acid-catalyzed epoxide cleavage of 1,4-naphthoquinone. This compound inhibits the SQR from *B. licheniformis* competitively with an IC_{50} value of 31 μ M.

Substrate Design, Synthesis, and Characterization. The determination of the electrogenicity of the catalysis of SQR required substrates that provide enough driving force for the catalyzed reaction to establish a Δp . A novel substrate analogue MMAN was designed and synthesized previously (16). The advantage of the MMAN/MMANH₂ couple is its lower redox potential compared to that of the DMN/DMNH₂ couple, ($\Delta E_m = -90$ mV (16)), thus increasing the ΔG of the reaction from $\Delta G \approx -12$ kJ/mol to $\Delta G \approx -30$ kJ/mol under standard conditions at pH 7 (16) and, in principle, providing sufficient driving force for the establishment of Δp in the direction of quinol oxidation by fumarate. Catalysis in the physiological direction (succinate oxidation by quinone) was monitored using either 2-ethyl-3-methyl-1,4-naphthoquinone (EMN) or 2,3-dimethoxy-5-ethyl-6-methyl-1,4-benzoquinone (EQ-0) as electron acceptors. The redox potential of the EMN/EMNH₂ couple is identical to that of the DMN/DMNH₂ couple, and that of the EQ-0/EQH₂-0 couple is 90 mV higher (shifting ΔG from $\Delta G \approx +12$ kJ/mol to $\Delta G \approx -6$ kJ/mol). Here, we report a new synthetic strategy for EQ-0, for which theoretical studies have been performed concerning its conformation (27), the prediction of EPR parameters of its radical anion (28), and its behavior inside a lipid bilayer (29).

Uncoupler-Stimulated Activity. In spite of supporting succinate oxidation by EMN in its detergent-solubilized state, when reconstituted into proteoliposomes, *B. licheniformis* SQR exhibited no detectable enzymatic activity of succinate oxidation by EMN (left part of Figure 4 and Table 2). We attributed this rapid loss in activity to the unfavorable difference in oxidation–reduction midpoint potential between the EMN/EMNH₂ couple and the fumarate/succinate couple, rendering the overall reaction mildly endergonic (see above) under standard conditions (at pH 7) and apparently not favorable enough, even with a large excess of educt versus product, to support sustained Δp generation. Repeating the

experiment in the presence of partially inhibiting concentrations (30 μ M) of HNN (blue line in Supporting Information, Figure S1) revealed an initial activity in the case of sealed proteoliposomes (Table 2), indicating that the reaction in the absence of inhibitor had reached equilibrium too quickly for us to monitor it in the present experimental setup. These conclusions are supported by our finding that the addition of the protonophore carbonyl cyanide *m*-chlorophenylhydrazone (CCCP) to ostensibly inactive proteoliposomal *B. licheniformis* SQR enabled the catalysis of EMN reduction (Table 2; right part of Figure 4). This effect could be inhibited by the addition of 60 μ M HNN (gray trace in Figure 4).

Generation of $\Delta\Psi$ and ΔpH . Two components contribute to Δp . These are the concentration differences of protons across the membrane, ΔpH , and the difference in electrical potential between the two membrane-separated aqueous phases, $\Delta\Psi$. Fumarate reduction by MMANH₂ as catalyzed by proteoliposomal *B. licheniformis* SQR generated a ΔpH of 1.2 pH units (Figures 5A and B; Table 3). The H^+/e^- ratio was 0.8. In the opposite direction, EQ-0 reduction by succinate resulted in a ΔpH of 1.8 pH units (Figures 5C and D; Table 3) with a H^+/e^- ratio of 0.9. The H^+/e^- ratios determined are only slightly lower than the theoretically expected value of 1, and the ΔpH values clearly support the scheme depicted in Figure 1. Both the quinone reductase activity as well as the ΔpH generation could be abolished by the addition of the competitive inhibitor HNN. No generation of a ΔpH could be detected with DMN and DMNH₂ as respective electron donor or acceptor.

We also determined the generation of $\Delta\Psi$ using the respective substrate couples same as those for ΔpH determination. Here, we measured a $\Delta\Psi$ of 72 mV (positive inside) upon oxidation of MMANH₂ by fumarate (Figure 6A) and a $\Delta\Psi$ of 184 mV (negative inside) in the physiological direction, succinate oxidation by EQ-0 reduction (Figure 6B). These values also clearly support the scheme depicted in Figure 1. No accumulation of TPP⁺ of TPB[−] could be detected with DMN and DMNH₂ as respective electron donor or acceptor (Table 4).

A comparison of the results obtained with the modified quinones with altered redox properties (MMANH₂, EQ-0) to the inability of proteoliposome-reconstituted *B. licheni-*

Table 4: TPP⁺ and TPB⁻ Accumulation by Proteoliposomes in the Steady State of Electron Transport

substrate quinol/quinone	direction of e^- transfer	reporter ion used	T_s (mM/g PL)	T_i (μ M)	T_e (μ M)	$\Delta\Psi$ (mV)
MMANH ₂	fumarate reduction	TPB ⁻	2.6	237	11.4	72
DMNH ₂	fumarate reduction	TPB ⁻ /TPP ⁺			3000	0
EQ-0	succinate oxidation	TPP ⁺	2.9	159	0.1	184

^a Proteoliposomes containing SQR were provided with different quinone/quinol substrates, as indicated in the first column.

formis SQR to support either DMN reduction or DMNH₂ oxidation without a supporting electrochemical potential demonstrates that this observation is due to the insufficient redox potential difference between the DMN/DMNH₂ and the fumarate/succinate couple. In conclusion, the experimental data presented here provide strong evidence that diheme-containing SQRs from Gram-positive bacteria exploit Δp to support the otherwise thermodynamically unfavorable oxidation of succinate by menaquinone. We have demonstrated that these effects are specifically associated with the activity of SQR.

ACKNOWLEDGMENT

We thank T. Zaunmüller and H. Claus for their assistance in growing *B. licheniformis* cells, T. Prisner for access to the cyclic voltammetry equipment, and B. Trumpower for providing an initial sample of HNN.

SUPPORTING INFORMATION AVAILABLE

Close-up of Figure 4 of the kinetic phase prior to the addition of uncoupler CCCP and a Table summarizing a comparative screening procedure for a suitable model organism. This material is available free of charge via the Internet at <http://pubs.acs.org>.

REFERENCES

- Hägerhäll, C. (1997) Succinate:quinone oxidoreductases. Variations on a conserved theme, *Biochim. Biophys. Acta* 1320, 107–141.
- Lancaster, C. R. D. (2002) Succinate:quinone oxidoreductases: an overview, *Biochim. Biophys. Acta* 1553, 1–6.
- Ohnishi, T., Moser, C. C., Page, C. C., Dutton, P. L., and Yano, T. (2000) Simple redox-linked proton-transfer design: new insights from structures of quinol:fumarate reductase, *Structure* 8, R23–R32.
- Lemma, E., Hägerhäll, C., Geisler, V., Brandt, U., von Jagow, G., and Kroger, A. (1991) Reactivity of the *Bacillus subtilis* succinate dehydrogenase complex with quinones, *Biochim. Biophys. Acta* 1059, 281–285.
- Collins, M. D., and Jones, D. (1981) Distribution of isoprenoid quinone structural types in bacteria and their taxonomic implications, *Microbiol. Rev.* 45, 316–354.
- Thauer, R. K., Jungermann, K., and Decker, K. (1977) Energy conservation in chemotrophic anaerobic bacteria, *Bacteriol. Rev.* 41, 100–180.
- Lemma, E., Uden, G., and Kröger, A. (1990) Menaquinone is an obligatory component of the chain catalyzing succinate respiration in *Bacillus subtilis*, *Arch. Microbiol.* 155, 62–67.
- Schirawski, J., and Uden, G. (1998) Menaquinone-dependent succinate dehydrogenase of bacteria catalyzes reversed electron transport driven by the proton potential, *Eur. J. Biochem.* 257, 210–215.
- Zaunmüller, T., Kelly, D. J., Glöckner, F. O., and Uden, G. (2006) Succinate dehydrogenase functioning by a reverse redox loop mechanism and fumarate reductase in sulphate-reducing bacteria, *Microbiology* 152, 2443–2453.
- Matsson, M., Tolstoy, D., Aasa, R., and Hederstedt, L. (2000) The distal heme center in *Bacillus subtilis* succinate:quinone reductase is crucial for electron transfer to menaquinone, *Biochemistry* 39, 8617–8624.
- Hägerhäll, C., and Hederstedt, L. (1996) A structural model for the membrane-integral domain of succinate:quinone oxidoreductases, *FEBS Lett.* 389, 25–31.
- Lancaster, C. R. D., Gross, R., Haas, A., Ritter, M., Mäntele, W., Simon, J., and Kröger, A. (2000) Essential role of Glu-C66 for menaquinol oxidation indicates transmembrane electrochemical potential generation by *Wolinella succinogenes* fumarate reductase, *Proc. Natl. Acad. Sci. U.S.A.* 97, 13051–13056.
- Schnorpfel, M., Janausch, I. G., Biel, S., Kröger, A., and Uden, G. (2001) Generation of a proton potential by succinate dehydrogenase of *Bacillus subtilis* functioning as a fumarate reductase, *Eur. J. Biochem.* 268, 3069–3074.
- Azarkina, N., and Konstantinov, A. A. (2002) Stimulation of menaquinone-dependent electron transfer in the respiratory chain of *Bacillus subtilis* by membrane energization, *J. Bacteriol.* 184, 5339–5347.
- White, P. J. (1972) The nutrition of *Bacillus megaterium* and *Bacillus cereus*, *J. Gen. Microbiol.* 132, 431–442.
- Madej, M. G., Nasiri, H. R., Hilgendorff, N. S., Schwalbe, H., and Lancaster, C. R. D. (2006) Evidence for transmembrane proton transfer in a dihaem-containing membrane protein complex, *EMBO J.* 25, 4963–4970.
- Biel, S., Simon, J., Gross, R., Ruiz, T., Ruitenber, M., and Kröger, A. (2002) Reconstitution of coupled fumarate respiration in liposomes by incorporating the electron transport enzymes isolated from *Wolinella succinogenes*, *Eur. J. Biochem.* 269, 1974–1983.
- Kita, K., Vibat, C. R. T., Meinhardt, S., Guest, J. R., and Gennis, R. B. (1989) One-step purification from *Escherichia coli* of complex II (succinate:ubiquinone oxidoreductase) associated with succinate-reducible cytochrome b556, *J. Biol. Chem.* 264, 2672–2677.
- Lancaster, C. R. D., Sauer, U. S., Gross, R., Haas, A. H., Graf, J., Schwalbe, H., Mäntele, W., Simon, J., and Madej, M. G. (2005) Experimental support for the “E-pathway hypothesis” of coupled transmembrane e^- and H^+ transfer in dihemic quinol:fumarate reductase, *Proc. Natl. Acad. Sci. U.S.A.* 102, 18860–18865.
- Bendall, M. R., Doddrell, M., and Pegg, D. T. (1981) Editing of carbon-13 NMR spectra. 1. A pulse sequence for the generation of subspectra, *J. Am. Chem. Soc.* 103, 4603–4605.
- Hunsdiecker, H., and Hunsdiecker, C. (1942) Degradation of the salts of aliphatic acids by bromine, *Chem. Ber.* 75, 291–297.
- Veith, B., Herzberg, Ch. Steckel, S., Feesche, J., Maurer, K. H., Ehrenreich, P., Bäuml, S., Henne, A., Liesegang, H., Merkl, R., Ehrenreich, A., and Gottschalk, G. (2004) The complete genome sequence of *Bacillus licheniformis* DSM13, an organism with great industrial potential, *J. Mol. Biotechnol.* 7, 204–211.
- Lancaster, C. R. D., Kröger, A., Auer, M., and Michel, H. (1999) Structure of fumarate reductase from *Wolinella succinogenes* at 2.2 Å resolution, *Nature* 402, 377–385.
- Mileni, M., MacMillan, F., Tziatzios, C., Zwicker, K., Haas, A. H., Mäntele, W., Simon, J., and Lancaster, C. R. D. (2006) Heterologous production in *Wolinella succinogenes* and characterization of the quinol:fumarate reductase enzymes from *Helicobacter pylori* and *Campylobacter jejuni*, *Biochem. J.* 395, 191–201.
- Yankovskaya, V., Horsefield, R., Tornroth, S., Luna-Chavez, C., Miyoshi, H., Leger, C., Byrne, B., Cecchini, G., and Iwata, S. (2003) Architecture of succinate dehydrogenase and reactive oxygen species generation, *Science* 299, 700–704.
- Kurokawa, T., and Sakamoto, J. (2005) Purification and characterization of succinate:menaquinone oxidoreductase from *Corynebacterium glutamicum*, *Arch. Microbiol.* 183, 317–324.
- Himo, F., Babcock, G. T., and Eriksson, L. A. (1999) Conformational analysis of quinone anion radicals in photosystem II and photosynthetic bacteria, *J. Phys. Chem. A* 103, 3745–3749.
- Kacprzak, S., Kaupp, M., and MacMillan, F. (2006) Protein-cofactor interactions and EPR parameters for the Q_H quinone binding site of quinol oxidase. A density functional study, *J. Am. Chem. Soc.* 128, 5659–5671.
- Söderhäll, J. A., and Laaksonen, A. (2001) Molecular dynamics simulations of ubiquinone inside a lipid bilayer, *J. Phys. Chem. B* 105, 9308–9315.